Laguerre-SVD Reduced-Order Modeling

Luc Knockaert, *Member, IEEE,* and Daniël De Zutter, *Senior Member, IEEE*

***Abstract*—A reduced-order modeling method based on a system description in terms of orthonormal Laguerre functions, together with a Krylov subspace decomposition technique is presented. The link with Padé approximation, the block Arnoldi process and singular value decomposition (SVD) leads to a simple and stable implementation of the algorithm. Novel features of the approach include the determination of the Laguerre parameter as a function of bandwidth and testing the accuracy of the results in terms of both amplitude and phase.**

***Index Terms*—Laguerre functions, Padé approximation, reduced-order modeling, singular value decomposition.**

I. Introduction

Circuit simulation tasks, such as the accurate prediction of the behavior of large RLGC interconnects, generally require the solution of very large linear networks. Since the main point, from a communications and throughput point of view, is the behavior of the interconnect structure at user-defined ports over a given frequency range, it is of utmost importance to dispose of a reduced but accurate black-box model of the network as seen from the chosen ports. In recent years this has led to the development of reduced-order modeling techniques such as asymptotic waveform evaluation (AWE) [1], matrix Padé via Lanczos (MPVL) [2], [3], symmetric Padé via Lanczos (SyMPVL) [4], block Arnoldi [5], and passive reduced-order interconnect macromodeling (PRIMA) [6].

Though quite different in implementation and numerical stability, most of these algorithms tend to obtain a low-order Padé approximant [7] of the system transfer matrix via Krylov subspace modeling. Some of these techniques, such as SyMPVL and PRIMA, are provably passive, partly because the model reduction scheme can be interpreted in terms of congruence transformations [8]. In this paper we propose an algorithm based on the decomposition of the system transfer matrix into orthogonal scaled Laguerre functions [9]. The link with Padé approximation, the block Arnoldi process, and the singular value decomposition (SVD) [10] permits a simple and stable implementation of the algorithm. As in PRIMA and SyMPVL, the method is provably passive. The algorithm is applied to transmission lines, coupled transmission lines, and a PEEC circuit [11]. Part of the material in this paper was presented at the 1999 EPEP meeting in San Diego [12]. The novelty of the material added consists mainly of a discussion of all the features of the algorithm, the choice of the Laguerre parameter in connection with bandwidth, the accuracy of the results—not only in terms of the amplitude, but also of the phase as a function of frequency—and an explicit state space description of general coupled transmission line circuits.

Manuscript received June 15, 2000.

The authors are with INTEC-IMEC, B-9000 Gent, Belgium (e-mail: knokaert@intec.rug.ac.b).

Publisher Item Identifier S 0018-9480(00)07413-5.

II. The Laguerre Connection

Using any circuit-equation formulation method such as modified nodal analysis (MNA) [13], sparse tableau, etc. [14], a lumped, linear, time-invariant strictly passive [15] multiport circuit of order N can be described by the following system of first-order differential equations:

$$\boldsymbol{C}\dot{\boldsymbol{x}} = -\boldsymbol{G}\boldsymbol{x} + \boldsymbol{B}\boldsymbol{u} \tag{1}$$

$$\boldsymbol{y} = \boldsymbol{L}^T\boldsymbol{x}. \tag{2}$$

Here, the vector $\boldsymbol{x}$ represents the circuit variables, $\dot{\boldsymbol{x}}$ represents the time derivative of $\boldsymbol{x}$, the $N \times N$ matrix $\boldsymbol{G}$ represents the contribution of memoryless elements, such as resistors, the $N \times N$ matrix $\boldsymbol{C}$ represents the contribution from memory elements, such as capacitors and inductors, the vector $\boldsymbol{y}$ is the output of interest, and the vector $\boldsymbol{u}$ represents the excitations at the ports. Note that $\boldsymbol{L}^T$ stands for the transpose of $\boldsymbol{L}$.

Since we consider a multiport formulation with p ports, where in general $p \ll N$, the rectangular matrices $\boldsymbol{L}$ and $\boldsymbol{B}$ are of dimension $N \times p$. Moreover, as explained in [6], without loss of generality we can take $\boldsymbol{L} = \boldsymbol{B}$. However, for the sake of generality, we will maintain the separate $\boldsymbol{B}$ and $\boldsymbol{L}$ notation throughout this paper.

With unit impulse excitations at the ports and zero initial conditions, the Laplace transform of the circuit equations (1), (2) yields the $p \times p$ port transfer matrix

$$\boldsymbol{H}(s) = \boldsymbol{L}^T(\boldsymbol{G} + s\boldsymbol{C})^{-1}\boldsymbol{B} \tag{3}$$

and the corresponding $p \times p$ port impulse response matrix

$$\boldsymbol{h}(t) = \mathcal{L}^{-1}\boldsymbol{H}(s). \tag{4}$$

In most of the reduced-order modeling literature, model reduction strategies are based on Padé approximations of the transfer matrix by means of moment matching. The approach we advocate in this paper is the expansion of the impulse response matrix $\boldsymbol{h}(t)$ in scaled Laguerre functions [9], defined as

$$\phi_n^\alpha(t) = \sqrt{2\alpha}e^{-\alpha t}\ell_n(2\alpha t), \qquad n = 0, 1, \cdots \tag{5}$$

where α is a positive scaling parameter and $\ell_n(t)$ is the Laguerre polynomial

$$\ell_n(t) = \frac{e^t}{n!}\frac{d^n}{dt^n}(e^{-t}t^n). \tag{6}$$

It is known [16] that the sequence $\{\phi_n^\alpha(t)\}$ forms a uniformly bounded orthonormal basis for the Hilbert space $L_2(R_+)$.

Hence the impulse response matrix $\boldsymbol{h}(t)$ admits the Fourier–Laguerre expansion

$$\boldsymbol{h}(t) = \sum_{n=0}^{\infty} \boldsymbol{F}_n \phi_n^\alpha(t). \tag{7}$$

Since the Hardy space $\mathcal{H}_2$ [9] consisting of all analytic and square-integrable functions in the open right half-plane $\Re s > 0$ is the Laplace transform of $L_2(R_+)$, the sequence of Laplace transforms of the scaled Laguerre functions

$$\Phi_n^\alpha(s) = \mathcal{L}\phi_n^\alpha(t) = \frac{\sqrt{2\alpha}}{s+\alpha}\left(\frac{s-\alpha}{s+\alpha}\right)^n, \qquad n = 0, 1, \cdots \tag{8}$$

forms a uniformly bounded orthonormal basis for the Hardy space $\mathcal{H}_2$ equipped with the inner product

$$\langle f|g\rangle = \frac{1}{2\pi}\int_{-\infty}^{\infty} f(i\omega)g^*(i\omega)\,d\omega \tag{9}$$

and norm $\nu(f) = \sqrt{\langle f|f\rangle}$.

Considering that the multiport circuit under scrutiny is strictly passive and hence asymptotically stable, and since the transfer matrix is strictly proper, i.e.,

$$\lim_{|s|\to\infty} |H_{ij}(s)| = 0, \qquad i, j = 1, \cdots, p \tag{10}$$

all the entries $H_{ij}(s)$ of $\boldsymbol{H}(s)$ belong to $\mathcal{H}_2$ and the transfer matrix can be expanded into the orthonormal basis $\{\Phi_n^\alpha(s)\}$ as

$$\boldsymbol{H}(s) = \boldsymbol{L}^T(\boldsymbol{G} + s\boldsymbol{C})^{-1}\boldsymbol{B} = \sum_{n=0}^{\infty} \boldsymbol{F}_n \Phi_n^\alpha(s). \tag{11}$$

This can be rewritten as

$$\boldsymbol{L}^T(\boldsymbol{G} + s\boldsymbol{C})^{-1}\boldsymbol{B} = \frac{\sqrt{2\alpha}}{s+\alpha}\sum_{n=0}^{\infty} \boldsymbol{F}_n\left(\frac{s-\alpha}{s+\alpha}\right)^n. \tag{12}$$

Equation (12) has the very simple physical interpretation that any transfer matrix in $\mathcal{H}_2$ can be represented as the product of a simple low-pass filter $\sqrt{2\alpha}/(s+\alpha)$ and a weighted infinite sum of all-pass filters of the type $[(s-\alpha)/(s+\alpha)]^n$. Moreover, the bilinear transformation

$$u = \frac{s-\alpha}{s+\alpha} \tag{13}$$

maps the s-domain Laguerre expansion (12) into the u-domain power expansion

$$\boldsymbol{L}^T([\alpha\boldsymbol{C} + \boldsymbol{G}] + u[\alpha\boldsymbol{C} - \boldsymbol{G}])^{-1}\boldsymbol{B} = \frac{1}{\sqrt{2\alpha}}\sum_{n=0}^{\infty} \boldsymbol{F}_n u^n. \tag{14}$$

From this we infer that an mth-order Padé approximation of the modified transfer matrix

$$\hat{\boldsymbol{H}}(u) = \boldsymbol{L}^T([\alpha\boldsymbol{C} + \boldsymbol{G}] + u[\alpha\boldsymbol{C} - \boldsymbol{G}])^{-1}\boldsymbol{B} \tag{15}$$

in the u-domain is equivalent to a an mth-order Laguerrre approximation in the s-domain, meaning that $\boldsymbol{H}(s)$ can be optimally approximated in the $\mathcal{H}_2$ norm sense by the truncated Fourier–Laguerre expansion

$$\boldsymbol{H}(s) \approx \sum_{n=0}^{m} \boldsymbol{F}_n \Phi_n^\alpha(s) = \boldsymbol{H}_m(s). \tag{16}$$

Although we know that $\boldsymbol{H}_m(s)$ converges to $\boldsymbol{H}(s)$ for $m \to \infty$ when $\Re s > 0$ for a strictly passive system, it is necessary, in order to be able to determine an adequate value for the Laguerre parameter α, to have more information about the convergence rate. We start with the partial fraction expansion

$$\boldsymbol{H}(s) = \sum_{k=1}^{N} \frac{\boldsymbol{h}_k}{s + v_k} \tag{17}$$

which is valid for simple poles $-v_k$ with $\Re v_k > 0$. It is readily shown that

$$\sum_{n=0}^{\infty} \Phi_n^\alpha(s)\Phi_n^\alpha(v) = \frac{1}{s+v} \qquad \text{for } \Re v > 0, \quad \Re s \geq 0. \tag{18}$$

It is interesting to note that the time-domain version of (18), obtained by taking the inverse Laplace transforms with respect to s *and* v, reads as

$$\sum_{n=0}^{\infty} \phi_n^\alpha(t)\phi_n^\alpha(t') = \delta(t - t') \qquad \text{for } t > 0, \quad t' > 0 \tag{19}$$

which is the reproducing kernel identity for the Laguerre functions. Identity (19) clearly indicates that even a pure time delay can be approximated by a Laguerre-type expansion. From (17) and (18) we obtain that

$$\boldsymbol{F}_n = \sum_{k=1}^{N} \boldsymbol{h}_k \Phi_n^\alpha(v_k). \tag{20}$$

Hence, with respect to any matrix norm $||\cdot||$, we have

$$||\boldsymbol{H}(i\omega) - \boldsymbol{H}_m(i\omega)|| \leq \sqrt{\frac{2\alpha}{\omega^2 + \alpha^2}} \sum_{k=m+1}^{\infty} ||\boldsymbol{F}_k|| \tag{21}$$

and in the light of (20) and (8)

$$||\boldsymbol{H}(i\omega) - \boldsymbol{H}_m(i\omega)|| \leq \frac{2\alpha}{\sqrt{\omega^2 + \alpha^2}} \sum_{k=1}^{N} \frac{||h_k||}{|v_k + \alpha| - |v_k - \alpha|}\left|\frac{v_k - \alpha}{v_k + \alpha}\right|^{m+1}. \tag{22}$$

For a strictly passive system, this proves the pointwise convergence $\boldsymbol{H}_m(i\omega) \to \boldsymbol{H}(i\omega)$ as m approaches infinity. It is seen that the overall convergence rate is dictated by the largest coefficient $|(v_k - \alpha)/(v_k + \alpha)|$ and hence the optimal α may be found as the solution to the minimax problem

$$\alpha = \arg\min_{\alpha > 0} \max_{1 \leq k \leq N} \left|\frac{v_k - \alpha}{v_k + \alpha}\right|. \tag{23}$$

It should be noted that the optimal α thus obtained is also the value that maximizes the radius of convergence of the power series in the r.h.s of (14), in agreement with the asymptotic theory developed in [17]. Since the minimum of $|(v-\alpha)/(v+\alpha)|$ is obtained for $\alpha=|v|$, it is a simple matter to show that the solution of the minimax problem (23) is given by $\alpha=|v_j|$, where j is the solution to the discrete minimax problem

$$j=\arg\min_{1\le j\le N}\max_{1\le k\le N}\left|\frac{v_k-|v_j|}{v_k+|v_j|}\right|. \tag{24}$$

It has been indicated in [2] and [18] that $\alpha\approx 2\pi B$, where B is the bandwidth of the system. The relationship between the Laguerre parameter α and the bandwidth B can be understood as follows: suppose we truncate the Fourier–Laguerre expansion of the impulse response matrix $\boldsymbol{h}(t)$ to m terms, i.e.,

$$\boldsymbol{h}(t)=\sum_{n=0}^{m-1}\boldsymbol{F}_n\phi_n^\alpha(t). \tag{25}$$

The coefficients $\boldsymbol{F}_n$ can be obtained by means of the discrete Laguerre transform [19] as

$$\boldsymbol{F}_n=\frac{1}{\sqrt{2\alpha}}\sum_{k=1}^{m}w_k\ell_n(t_k)e^{t_k/2}\boldsymbol{h}(t_k/2\alpha) \tag{26}$$

where the w_k, t_k are the weights and nodes—zeros of $\ell_m(t)$—of the m-point Gauss–Laguerre quadrature rule [20]. This means that in order to retain m Laguerre coefficients, the impulse response needs to be known up to a time $T\approx t_m/2\alpha$, where t_m is the largest zero of $\ell_m(t)$. For m large we have asymptotically [21] $t_m\approx 4m$—for example calculations based on [20] yield $t_{10\,000}=39\,875.146$—and hence $T\approx 2m/\alpha$. By virtue of the $2WT$ theorem of Slepian [22] we must have $m\ge 2BT$ or $\alpha\ge 4B$. If we take $2\pi B$ as the geometric mean of the bounds on α we can propose the range

$$4B\le\alpha\le\pi^2B \tag{27}$$

containing "good" values for the Laguerre parameter. This shows that there is some leeway in choosing α, as long as it is not too "close" to zero or infinity. Note that, following the definition (5) of the scaled Laguerre functions, the optimal Laguerre parameter can be interpreted as the reciprocal of the time constant of the system, i.e., $\alpha=1/\tau$, and hence the inequalities (27) represent upper and lower bounds for the bandwidth-time constant product $B\tau$.

Remark 1: Note that the conformal transformation (13) maps the open right half-plane $\Re s>0$ onto the open unit disk $|u|<1$. It has been shown [23] that there exists a profound relationship between complete orthonormal bases (COB), such as the Laguerre basis, and conformal Riemann mappings from simply connected regions onto the unit disk. One such COB, related to the trivial mapping $f(z)=z$ of the unit disk onto itself, is simply the set of monomials $\{z^n\}$ and hence Padé approximation inside the unit circle can be thought of as a projection technique on this simple COB. On the other hand, the set of monomials $\{s^n\}$ in the Laplace domain $\Re s>0$ is certainly not a COB there, but the Laguerre basis $\{\Phi_n^\alpha(s)\}$ presents one of the simplest bases, related to the conformal mapping $f(s)=(s-\alpha)/(s+\alpha)$. In a sense we can say that the Laguerre technique in the Laplace domain is equivalent to the Padé technique inside the unit circle. A single-input/single-output (SISO) reduced-order modeling strategy presented recently [24] developed more or less the same idea, although without explicit reference to the Laguerre COB, but with an actual Laguerre parameter $\alpha=1$. A major difference with the approach in [24] and our approach, is that α is in fact related to the bandwidth of the system—see (27).

III. The Krylov-SVD Connection

Defining the matrices

$$\boldsymbol{A}=-\boldsymbol{G}^{-1}\boldsymbol{C}\quad\text{and }\boldsymbol{R}=\boldsymbol{G}^{-1}\boldsymbol{B} \tag{28}$$

it is shown in [6] that the column-orthogonal matrix $\boldsymbol{X}$ associated with the block Arnoldi process [5] in order to orthogonalize the columns of the $N\times pq$ Krylov matrix

$$\boldsymbol{K}_q=[\boldsymbol{R},\,\boldsymbol{AR},\,\boldsymbol{A}^2\boldsymbol{R},\,\cdots,\,\boldsymbol{A}^{q-1}\boldsymbol{R}] \tag{29}$$

yields a reduced-order system

$$\tilde{\boldsymbol{C}}\dot{\boldsymbol{x}}=-\tilde{\boldsymbol{G}}\boldsymbol{x}+\tilde{\boldsymbol{B}}\boldsymbol{u} \tag{30}$$

$$\boldsymbol{y}=\tilde{\boldsymbol{L}}^T\boldsymbol{x} \tag{31}$$

with

$$\tilde{\boldsymbol{C}}=\boldsymbol{X}^T\boldsymbol{C}\boldsymbol{X},\quad\tilde{\boldsymbol{G}}=\boldsymbol{X}^T\boldsymbol{G}\boldsymbol{X},\quad\tilde{\boldsymbol{B}}=\boldsymbol{X}^T\boldsymbol{B},\quad\tilde{\boldsymbol{L}}=\boldsymbol{X}^T\boldsymbol{L} \tag{32}$$

such that the reduced-order transfer matrix

$$\tilde{\boldsymbol{H}}(s)=\tilde{\boldsymbol{L}}^T\left(\tilde{\boldsymbol{G}}+s\tilde{\boldsymbol{C}}\right)^{-1}\tilde{\boldsymbol{B}} \tag{33}$$

is a passive Padé approximant of order $q-1$ for the original transfer matrix.

By virtue of the preceding section, the above reasoning remains valid, in the sense of Laguerre approximation, if we define the modified system matrices

$$\hat{\boldsymbol{A}}=-(\alpha\boldsymbol{C}+\boldsymbol{G})^{-1}(\alpha\boldsymbol{C}-\boldsymbol{G})\quad\text{and }\hat{\boldsymbol{R}}=(\alpha\boldsymbol{C}+\boldsymbol{G})^{-1}\boldsymbol{B}. \tag{34}$$

In other words, we assert that the column-orthogonal matrix $\hat{\boldsymbol{X}}$ associated with the block Arnoldi process as applied to the $N\times pq$ modified Krylov matrix

$$\hat{\boldsymbol{K}}_q=\left[\hat{\boldsymbol{R}},\,\hat{\boldsymbol{A}}\hat{\boldsymbol{R}},\,\hat{\boldsymbol{A}}^2\hat{\boldsymbol{R}},\,\cdots,\,\hat{\boldsymbol{A}}^{q-1}\hat{\boldsymbol{R}}\right] \tag{35}$$

yields a reduced-order system described by

$$\tilde{\boldsymbol{C}}=\hat{\boldsymbol{X}}^T\boldsymbol{C}\hat{\boldsymbol{X}},\quad\tilde{\boldsymbol{G}}=\hat{\boldsymbol{X}}^T\boldsymbol{G}\hat{\boldsymbol{X}},\quad\tilde{\boldsymbol{B}}=\hat{\boldsymbol{X}}^T\boldsymbol{B},\quad\tilde{\boldsymbol{L}}=\hat{\boldsymbol{X}}^T\boldsymbol{L} \tag{36}$$

such that the reduced-order transfer matrix

$$\tilde{\boldsymbol{H}}(s)=\tilde{\boldsymbol{L}}^T\left(\tilde{\boldsymbol{G}}+s\tilde{\boldsymbol{C}}\right)^{-1}\tilde{\boldsymbol{B}} \tag{37}$$

is a passive Laguerre approximant of order $q-1$ for the original transfer matrix.

The block Arnoldi algorithm (BAA) [5] can be utilized to generate the column-orthogonal matrix $\hat{\boldsymbol{X}}$. Equivalently we can use a block "thin" QR factorization based on modified Gram–Schmidt (MGS) orthogonalization [10]. Numerical experience [5], [25] has shown that some steps in BAA have to be repeated in order to ensure orthogonality to the precision of the computer. To avoid this, we opt for an SVD based technique, which is a numerically more stable algorithm than MGS [26]. The idea behind the SVD approach is the following.

Putting $r = pq < N$, the dimension of the Krylov matrix $\hat{\boldsymbol{K}}_q$ is $N \times r$. Since BAA is equivalent to MGS, we compare the SVD and the "thin" QR factorization of $\hat{\boldsymbol{K}}_q$. We have

$$\hat{\boldsymbol{K}}_q = \hat{\boldsymbol{X}}\boldsymbol{R}_t = \boldsymbol{U}\Sigma\boldsymbol{V}^T \tag{38}$$

where

- $\hat{\boldsymbol{X}}, \boldsymbol{U}$ — $N \times r$ column-orthogonal matrices;
- $\boldsymbol{R}_t$ — $r \times r$ upper triangular matrix;
- Σ — $r \times r$ diagonal matrix containing the singular values of the Krylov matrix;
- $\boldsymbol{V}$ — $r \times r$ orthogonal matrix.

Since $\hat{\boldsymbol{X}}^T\hat{\boldsymbol{X}} = \boldsymbol{U}^T\boldsymbol{U} = \boldsymbol{I}_r$, it is easily seen that $\hat{\boldsymbol{X}}$ can be written as $\hat{\boldsymbol{X}} = \boldsymbol{U}\boldsymbol{Q}$, where $\boldsymbol{Q}$ is an $r \times r$ orthogonal matrix. From (36) and (37) we infer that the reduced-order model transfer matrix can be written as

$$\tilde{\boldsymbol{H}}(s) = \boldsymbol{L}^T\hat{\boldsymbol{X}}\left(\hat{\boldsymbol{X}}^T(\boldsymbol{G}+s\boldsymbol{C})\hat{\boldsymbol{X}}\right)^{-1}\hat{\boldsymbol{X}}^T\boldsymbol{B} \tag{39}$$

$$= \boldsymbol{L}^T\boldsymbol{U}\boldsymbol{Q}(\boldsymbol{Q}^T\boldsymbol{U}^T(\boldsymbol{G}+s\boldsymbol{C})\boldsymbol{U}\boldsymbol{Q})^{-1}\boldsymbol{Q}^T\boldsymbol{U}^T\boldsymbol{B} \tag{40}$$

$$= \boldsymbol{L}^T\boldsymbol{U}(\boldsymbol{U}^T(\boldsymbol{G}+s\boldsymbol{C})\boldsymbol{U})^{-1}\boldsymbol{U}^T\boldsymbol{B}. \tag{41}$$

Note that the mere requirement that $\boldsymbol{Q}$ is nonsingular is sufficient to obtain result (41). The derivations (39)–(41) prove that it is judicious to use the left SVD column-orthogonal factor $\boldsymbol{U}$ instead of $\hat{\boldsymbol{X}}$ in the reduced-order modeling scheme.

The complete SVD-Laguerre-based algorithm is constructed as follows.

- Select the values for α and q.
- Solve $(\boldsymbol{G}+\alpha\boldsymbol{C})\hat{\boldsymbol{R}}_0 = \boldsymbol{B}$.
- For $k = 1, \cdots, q-1$ solve $(\boldsymbol{G}+\alpha\boldsymbol{C})\hat{\boldsymbol{R}}_k = (\boldsymbol{G}-\alpha\boldsymbol{C})\hat{\boldsymbol{R}}_{k-1}$.
- $\boldsymbol{U}\Sigma\boldsymbol{V}^T = \mathrm{SVD}[\hat{\boldsymbol{R}}_0, \hat{\boldsymbol{R}}_1, \cdots, \hat{\boldsymbol{R}}_{q-1}]$.
- $\tilde{\boldsymbol{C}} = \boldsymbol{U}^T\boldsymbol{C}\boldsymbol{U}\ \tilde{\boldsymbol{G}} = \boldsymbol{U}^T\boldsymbol{G}\boldsymbol{U}\ \tilde{\boldsymbol{B}} = \boldsymbol{U}^T\boldsymbol{B}\ \tilde{\boldsymbol{L}} = \boldsymbol{U}^T\boldsymbol{L}$.

It is also important to evaluate $\boldsymbol{H}(s)$ or $\tilde{\boldsymbol{H}}(s)$ explicitly as a sum of partial fractions. Taking s_0 such that $\boldsymbol{G}+s_0\boldsymbol{C}$ is nonsingular, we have

$$\boldsymbol{H}(s) = \boldsymbol{L}^T(\boldsymbol{G}+s_0\boldsymbol{C}+(s-s_0)\boldsymbol{C})^{-1}\boldsymbol{B}$$

$$= \boldsymbol{L}^T(\boldsymbol{I}+(s-s_0)\boldsymbol{E})^{-1}\boldsymbol{B}_0 \tag{42}$$

where

$$\boldsymbol{E} = (\boldsymbol{G}+s_0\boldsymbol{C})^{-1}\boldsymbol{C}, \qquad \boldsymbol{B}_0 = (\boldsymbol{G}+s_0\boldsymbol{C})^{-1}\boldsymbol{B}. \tag{43}$$

Supposing $\boldsymbol{E}$ nondefective, i.e., diagonalizable, admits the eigendecomposition

$$\boldsymbol{E} = \boldsymbol{P}\Lambda\boldsymbol{P}^{-1} \tag{44}$$

where Λ is a diagonal matrix, yielding the partial fraction expression

$$\boldsymbol{H}(s) = \boldsymbol{L}^T\boldsymbol{P}(\boldsymbol{I}+(s-s_0)\Lambda)^{-1}\boldsymbol{P}^{-1}\boldsymbol{B}_0. \tag{45}$$

To avoid supplementary LU-decomposition overhead, it can be naturally recommended to choose the parameter s_0 equal to α.

Remark 2: As was shown in the derivation leading to (41), any decomposition of the Krylov matrix of the form $\hat{\boldsymbol{K}}_q = \boldsymbol{U}\boldsymbol{Z}$, where $\boldsymbol{U}$ is column orthogonal and $\boldsymbol{Z}$ is nonsingular, leads to the same reduced transfer matrix. Hence it is useful to compare the computational complexity (flop count) of the three major methods which carry this out: MGS, SVD, and Householder QR (HQR). The flop counts [10] are respectively of the order $O(mn^2)$, $O(4m^2n)$, and $O(2mn^2)$, where m is the largest and n is the smallest dimension of the Krylov matrix. Hence, in terms of flop counts, MGS is the cheapest method, followed by HQR and SVD. However, when orthonormality is critical [10]—or equivalently, if passivity is critical [8]—the order of the three methods must be reversed, i.e., first SVD, next HQR, and finally MGS. So each of these methods has its own merits in terms of efficiency and robustness. Also it seems that HQR is a tempting method for future research, especially as there exist specific updating algorithms [26]. An additional advantage of the Laguerre-based method is that the relevant condition number is not $\mathrm{cond}(\boldsymbol{G})$, but $\mathrm{cond}(\boldsymbol{G}+\alpha\boldsymbol{C})$; e.g., for the third example (PEEC circuit) we found typically that $\mathrm{cond}(\boldsymbol{G}+\alpha\boldsymbol{C}) < 0.01 * \mathrm{cond}(\boldsymbol{G})$.

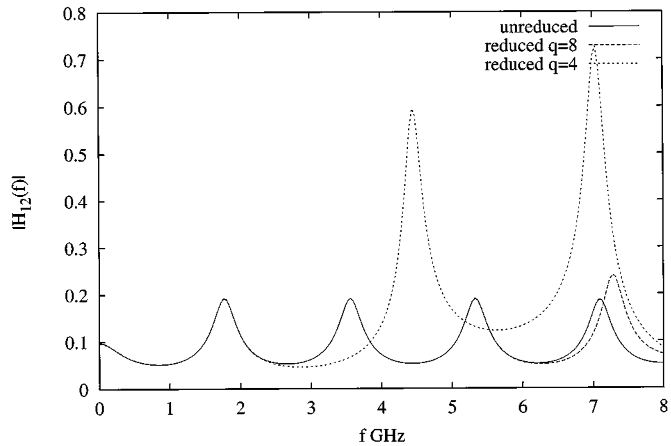

Fig. 1. $|H_{12}(f)|$ for the lossy transmission line.

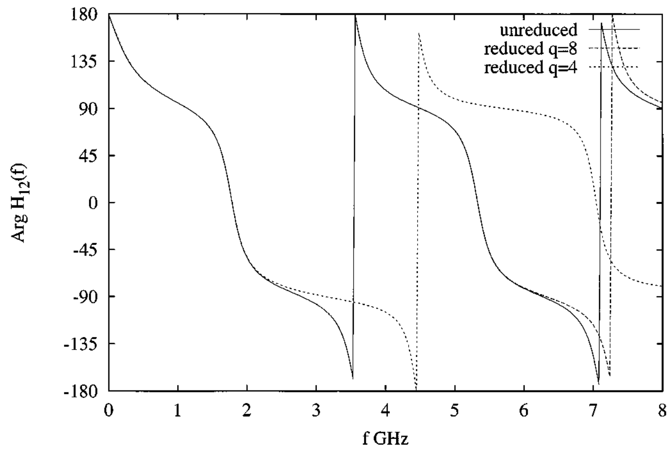

Fig. 2. $\arg H_{12}(f)$ for the lossy transmission line.

IV. Numerical Simulations

A. Lossy Transmission Line

Consider a lossy transmission line modeled by M lumped RLGC sections. The circuit equations for the corresponding $(p = 2)$ twoport are

$$C_n\frac{dv_n}{dt} = -G_nv_n + i_n - i_{n+1}, \qquad n = 1, \cdots, M \tag{46}$$

$$L_n\frac{di_n}{dt} = -R_ni_n + v_{n-1} - v_n, \qquad n = 1, \cdots, M+1. \tag{47}$$

The input variables are $u_1 = v_0$, $u_2 = v_{M+1}$ and the output variables are $y_1 = i_1$, $y_2 = -i_{M+1}$. The state variables are the entries of the $N = 2M + 1$–dimensional vector

$$\boldsymbol{x} = (v_1, \cdots, v_M,\ i_1, \cdots, i_{M+1})^T. \tag{48}$$

The standard $\boldsymbol{C}$, $\boldsymbol{G}$, $\boldsymbol{B}$, $\boldsymbol{L}$ MNA format is easily derived. For example, when $M = 2$ we have

$$\underbrace{\begin{pmatrix} C_1 & 0 & 0 & 0 & 0 \\ 0 & C_2 & 0 & 0 & 0 \\ 0 & 0 & L_1 & 0 & 0 \\ 0 & 0 & 0 & L_2 & 0 \\ 0 & 0 & 0 & 0 & L_3 \end{pmatrix}}_{\boldsymbol{C}} \dot{\boldsymbol{x}} = -\underbrace{\begin{pmatrix} G_1 & 0 & -1 & 1 & 0 \\ 0 & G_2 & 0 & -1 & 1 \\ 1 & 0 & R_1 & 0 & 0 \\ -1 & 1 & 0 & R_2 & 0 \\ 0 & -1 & 0 & 0 & R_3 \end{pmatrix}}_{\boldsymbol{G}} \boldsymbol{x} + \underbrace{\begin{pmatrix} 0 & 0 \\ 0 & 0 \\ 1 & 0 \\ 0 & 0 \\ 0 & -1 \end{pmatrix}}_{\boldsymbol{B}} \boldsymbol{u} \tag{49}$$

and of course $\boldsymbol{L} = \boldsymbol{B}$. A choice of $M = 40$ equal RLGC sections as in [6] with total parameters $G_{\rm tot} = 0$, $R_{\rm tot} = 10$ Ω, $L_{\rm tot} = 5$ nH, $C_{\rm tot} = 15$ pF yields a system description of order $N = 81$. Reduced-order Laguerre models of dimensions $r = 2q = 8$ and $r = 2q = 16$ are constructed using $s_0 = \alpha = 2\pi 10^9$. Figs. 1 and 2 show $|H_{12}(f)|$ and $\arg H_{12}(f)$ versus their reduced-order counterparts. It is seen that the $q = 4$, $q = 8$ Laguerre reduced-order models are indistinguishable from the unreduced model up to respectively 2 and 6 GHz. It is important to note that both amplitude and phase are approximated with the same degree of accuracy, i.e., the deviation from the exact result starts at the same frequency for both amplitude and phase. This remark holds for all the other examples in the sequel.

B. Coupled Lossy Transmission Lines

Coupled lossy multiconductor transmission lines can easily be modeled by a multiport generalization of (46), (47). The circuit equations for M sections, obtained from the discretization of the coupled matrix telegrapher equations [27], can be written as

$$\boldsymbol{C}_n \frac{d\boldsymbol{v}_n}{dt} = -\boldsymbol{G}_n \boldsymbol{v}_n + \boldsymbol{i}_n - \boldsymbol{i}_{n+1} \qquad n = 1, \cdots, M \tag{50}$$

$$\boldsymbol{L}_n \frac{d\boldsymbol{i}_n}{dt} = -\boldsymbol{R}_n \boldsymbol{i}_n + \boldsymbol{v}_{n-1} - \boldsymbol{v}_n \qquad n = 1, \cdots, M+1 \tag{51}$$

where $\boldsymbol{v}_n$ and $\boldsymbol{i}_n$ are $c \times 1$ column vectors and $\boldsymbol{C}_n$, $\boldsymbol{L}_n$, $\boldsymbol{G}_n$, and $\boldsymbol{R}_n$ are $c \times c$ square matrices. The standard MNA format is then

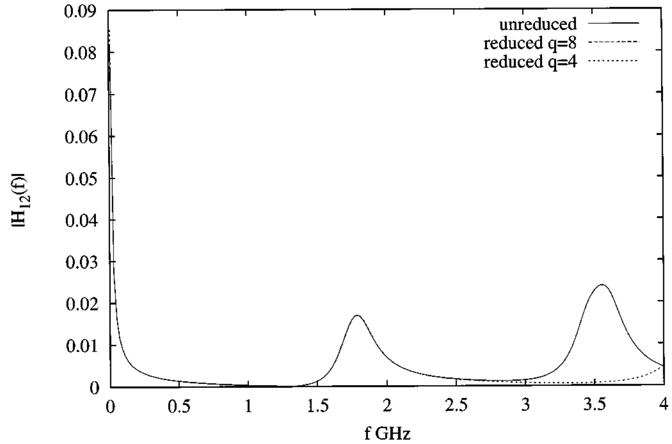

Fig. 3. $|H_{12}(f)|$ for the coupled lossy transmission lines.

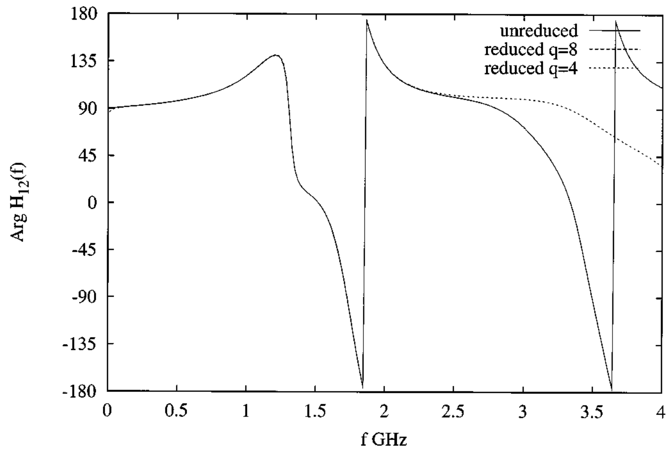

Fig. 4. $\arg H_{12}(f)$ for the coupled lossy transmission lines.

simply a block matrix generalization of (49), i.e., for $M = 2$ we have

$$\underbrace{\begin{pmatrix} \boldsymbol{C}_1 & 0 & 0 & 0 & 0 \\ 0 & \boldsymbol{C}_2 & 0 & 0 & 0 \\ 0 & 0 & \boldsymbol{L}_1 & 0 & 0 \\ 0 & 0 & 0 & \boldsymbol{L}_2 & 0 \\ 0 & 0 & 0 & 0 & \boldsymbol{L}_3 \end{pmatrix}}_{\boldsymbol{C}} \dot{\boldsymbol{x}} = -\underbrace{\begin{pmatrix} \boldsymbol{G}_1 & 0 & -\boldsymbol{I}_c & \boldsymbol{I}_c & 0 \\ 0 & \boldsymbol{G}_2 & 0 & -\boldsymbol{I}_c & \boldsymbol{I}_c \\ \boldsymbol{I}_c & 0 & \boldsymbol{R}_1 & 0 & 0 \\ -\boldsymbol{I}_c & \boldsymbol{I}_c & 0 & \boldsymbol{R}_2 & 0 \\ 0 & -\boldsymbol{I}_c & 0 & 0 & \boldsymbol{R}_3 \end{pmatrix}}_{\boldsymbol{G}} \boldsymbol{x} + \underbrace{\begin{pmatrix} 0 & 0 \\ 0 & 0 \\ \boldsymbol{I}_c & 0 \\ 0 & 0 \\ 0 & -\boldsymbol{I}_c \end{pmatrix}}_{\boldsymbol{B}} \boldsymbol{u} \tag{52}$$

where $\boldsymbol{I}_c$ is the $c \times c$ identity matrix. It is seen that the MNA system order is $N = (2M + 1)c$ and the number of columns

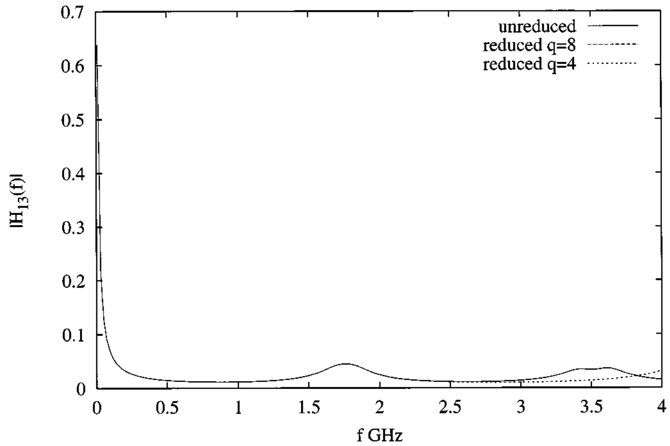

Fig. 5. $|H_{13}(f)|$ for the coupled lossy transmission lines.

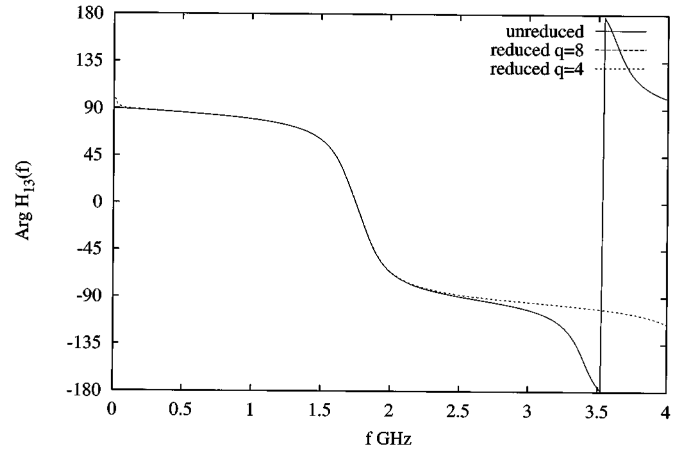

Fig. 6. $\arg H_{13}(f)$ for the coupled lossy transmission lines.

in $\boldsymbol{B} = \boldsymbol{L}$ is $p = 2c$. The discretized example of a 5-cm long four-port $(c = 2)$ multiconductor transmission line consisting of $M = 40$ equal sections with total matrices given by (extrapolated from the data in [27])

$$\boldsymbol{G}_{\text{tot}} = \begin{pmatrix} 0.005 & -0.0005 \\ -0.0005 & 0.005 \end{pmatrix} \text{S}$$
$$\boldsymbol{R}_{\text{tot}} = \begin{pmatrix} 0.005 & 0.001 \\ 0.001 & 0.005 \end{pmatrix} \Omega \tag{53}$$

and

$$\boldsymbol{L}_{\text{tot}} = \begin{pmatrix} 24.73 & 3.165 \\ 3.165 & 24.73 \end{pmatrix} \text{nH}$$
$$\boldsymbol{C}_{\text{tot}} = \begin{pmatrix} 3.14 & -0.245 \\ -0.245 & 3.14 \end{pmatrix} \text{pF} \tag{54}$$

yields a system description of order $N = 162$. Reduced-order Laguerre models of dimensions $r = 2cq = 16$ and $r = 2cq = 32$ are constructed using $s_0 = \alpha = 2\pi 10^9$. We observed that the symmetric transfer matrix $\boldsymbol{yH}(f)$ is Toeplitz, except for $H_{12}(f)$ which is only approximately equal to $H_{23}(f)$, and block-symmetric i.e., $H_{14}(f) = H_{23}(f)$. Figs. 3–6 show $|H_{12}(f)|$, $\arg H_{12}(f)$, $|H_{13}(f)|$, and $\arg H_{13}(f)$ versus their reduced-order counterparts up to 4 GHz. It is seen that the reduced-order models closely approximate the original model over the given frequency range. The results for $q = 8$ are even undistinguishable from the exact results.

C. A PEEC Circuit

As a third example we take the lumped-element equivalent circuit for a three-dimensional electromagnetic problem modeled via partial element equivalent circuit (PEEC) [11] as documented in [2]. The two-port $(p = 2)$ circuit consists of 2100 capacitors, 172 inductors, and 6990 inductive couplings, resulting in an MNA system of order $N = 306$. Reduced-order Laguerre models of dimensions $r = 2q = 60$ and $r = 2q = 90$ are constructed using $s_0 = \alpha = 10\pi 10^9$. Figs. 7 and 8 show $|H_{12}(f)|$ and $\arg H_{12}(f)$ versus their reduced-order counterparts. It is seen that the $q = 30$, $q = 45$ Laguerre reduced-order models are very close to the unreduced model up to respectively 2 and 4 GHz. We also simulated a reduced-order Laguerre model of dimension $r = 2q = 120$ and found it indistinguishable from the unreduced model over the 5-GHz frequency range.

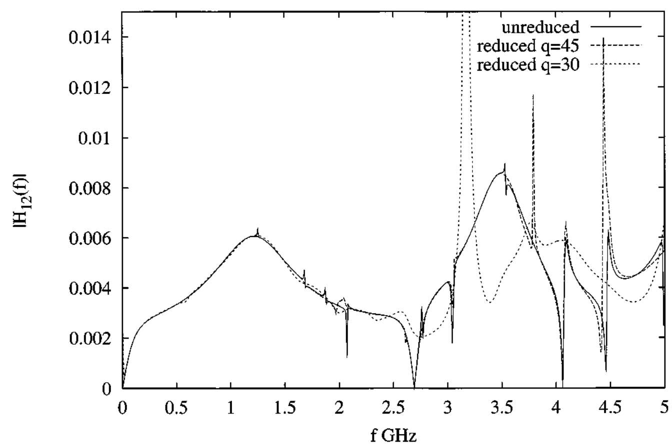

Fig. 7. $|H_{12}(f)|$ for the PEEC circuit.

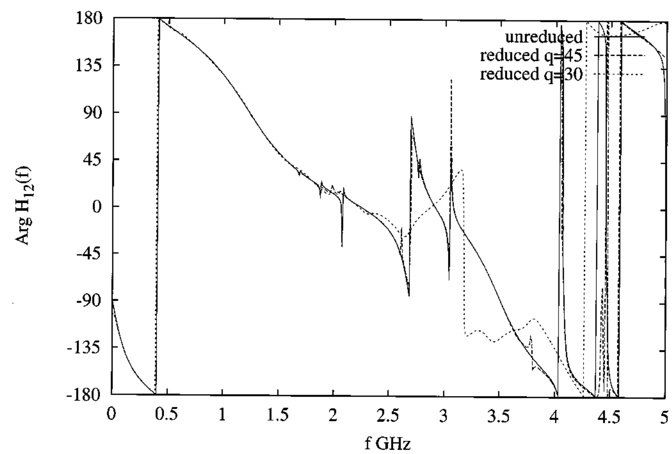

Fig. 8. $\arg H_{12}(f)$ for the PEEC circuit.

REFERENCES

[1] L. T. Pillage and R. A. Rohrer, "Asymptotic waveform evaluation for timing analysis," *IEEE Trans. Computer-Aided Design*, vol. 9, pp. 352–366, Apr. 1990.

[2] P. Feldmann and R. W. Freund, "Efficient linear circuit analysis by Padé approximation via the Lanczos process," *IEEE Trans. Computer-Aided Design*, vol. 14, pp. 639–649, May 1995.

[3] J. I. Aliaga, D. L. Boley, R. W. Freund, and V. Hernández, "A Lanczos-type method for multiple starting vectors," in *Numer. Anal. Manuscript*. Murray Hill, NJ: Bell Lab., Sept. 1998.

[4] R. W. Freund and P. Feldmann, "The SyMPVL algorithm and its applications to interconnect simulation," in *Numer. Anal. Manuscript*. Murray Hill, NJ: Bell Labs., June 1997.

[5] D. L. Boley, "Krylov space methods on state-space control models," *Circuits Syst. Signal Processing*, vol. 13, no. 6, pp. 733–758, 1994.

[6] A. Odabasioglu, M. Celik, and L. T. Pileggi, "PRIMA: Passive reduced-order interconnect macromodeling algorithm," *IEEE Trans. Computer-Aided Design*, vol. 17, pp. 645–654, Aug. 1998.

[7] A. Bultheel and M. Van Barel, "Padé techniques for model reduction in linear system theory: A survey," *J. Comput. Appl. Math.*, vol. 14, pp. 401–438, 1986.

[8] K. J. Kerns and A. T. Yang, "Preservation of passivity during RLC network reduction via split congruence transformations," *IEEE Trans. Computer-Aided Design*, vol. 17, pp. 582–591, July 1998.

[9] Z. Zang, A. Cantoni, and K. L. Teo, "Continuous-time envelope-constrained filter design via Laguerre filters and $\mathcal{H}_\infty$ optimization methods," *IEEE Trans. Signal Processing*, vol. 46, pp. 2601–2610, Oct. 1998.

[10] G. H. Golub and C. F. Van Loan, *Matrix Computations*. Baltimore, MD: Johns Hopkins, 1996.

[11] A. E. Ruehli, "Equivalent circuit models for three-dimensional multiconductor systems," *IEEE Trans. Microwave Theory Tech.*, vol. MTT-22, pp. 216–221, Mar. 1974.

[12] L. Knockaert and D. De Zutter, "Laguerre-SVD reduced order modeling," in *8th Topical Meeting on Electrical Performance of Electronic Packaging EPEP'99*, San Diego, CA, Oct. 1999, pp. 249–252.

[13] C.-W. Ho, A. E. Ruehli, and P. A. Brennan, "The modified nodal approach to network analysis," *IEEE Trans. Circuits Syst.*, vol. CAS-22, pp. 504–509, June 1975.

[14] J. Vlach and K. Singhal, *Computer Methods for Circuit Analysis and Design*. New York: Van Nostrand Reinholt, 1983.

[15] R. A. Rohrer and H. Nosrati, "Passivity considerations in stability studies of numerical integration algorithms," *IEEE Trans. Circuits Syst.*, vol. CAS-28, pp. 857–866, Sept. 1981.

[16] G. Szegö, "Orthogonal polynomials," in *Amer. Math. Soc. Coll. Publ.*, vol. 23, 1939.

[17] M. Schetzen, "Asymptotic optimum Laguerre series," *IEEE Trans. Circuit Theory*, vol. CT-18, pp. 493–500, Sept. 1971.

[18] L. Knockaert and D. De Zutter, "Passive reduced order multiport modeling: The Padé–Laguerre, Krylov–Arnoldi-SVD connection," *Arch. Elektron. Übertragungstech*, vol. 53, no. 5, pp. 254–260, 1999.

[19] G. Mandyam and N. Ahmed, "The discrete Laguerre transform: Derivation and applications," *IEEE Trans. Signal Processing*, vol. 44, pp. 2925–2931, Dec. 1996.

[20] W. Gautschi, "Algorithm 726: ORTHPOL—A package of routines for generating orthogonal polynomials and Gauss-type quadrature rules," *ACM Trans. Math. Software*, vol. 20, no. 1, pp. 21–62, Mar. 1994.

[21] H. Dette and W. J. Studden, "Some new asymptotic properties for the zeros of Jacobi, Laguerre and Hermite polynomials," *Constr. Approx.*, vol. 11, no. 2, pp. 227–238, 1995.

[22] D. Slepian, "On bandwidth," *Proc. IEEE*, vol. 64, pp. 292–300, Mar. 1976.

[23] L. Knockaert, "Orthonormal Riemann filter systems," in *Signal Processing Symposium SPS-2000*, Hilvarenbeek, The Netherlands, Mar. 2000, p. 7.

[24] C. Chen and D. F. Wong, "Error bounded Padé approximation via bilinear conformal transformation," in *36th Design Automation Conf. DAC'99*, New Orleans, LA, June 1999, Also on http://www.sigda.acm.org/Archives/ProceedingArchives, pp. 7–12.

[25] Y. Saad and M. H. Schultz, "GMRES: A generalized minimal residual algorithm for solving nonsymmetric linear systems," *SIAM J. Sci. Stat. Comput.*, vol. 7, no. 3, pp. 856–869, July 1986.

[26] W. H. Press, S. A. Teukolsky, W. T. Vetterling, and B. P. Flannery, *Numerical Recipes*. Cambridge, U.K.: Cambridge Univ. Press, 1992.

[27] A. R. Djordjević and T. K. Sarkar, "Analysis of time response of lossy multiconductor transmission line networks," *IEEE Trans. Microwave Theory Tech.*, vol. MTT-35, pp. 898–908, Oct. 1987.

Luc Knockaert (M'81) received the Physical Engineer, Telecommunications Engineer, and Ph. D. degrees in electrical engineering from the University of Gent, Belgium, in 1974, 1977, and 1987, respectively.

From 1979 to 1984 and from 1988 to 1995 he was working in North–South cooperation and development projects at the Universities of Congo and Burundi. He is presently a Senior Researcher at INTEC-IMEC. His current research interests are the application of statistical and linear algebra methods in signal identification, Shannon theory, matrix compression, reduced-order modeling, and the use of integral transforms in electromagnetic problem solving. As author or co-author he has contributed to more than 30 international journal papers.

Dr. Knockaert is a member of the Association for Computing Machinery (ACM).

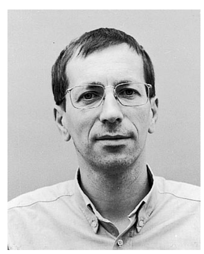

Daniël De Zutter (M'92–SM'96) was born in Eeklo, Belgium on November 8, 1953. He received a degree in electrical engineering from the University of Gent, Belgium in July 1976. In October 1981 he received the Ph.D. degree and in the spring of 1984 he completed a thesis leading to a degree equivalent to the French Aggrégation or the German Habilitation.

From September 1976 to September 1984 he was a Research and Teaching Assistant in the Laboratory of Electromagnetism and Acoustics (now the Department of Information Technology) at the same university. He is now a Full Professor at the Department of Information Technology, University of Gent. Most of his earlier scientific work dealt with the electrodynamics of moving media, with emphasis on the Doppler effect and on Lorentz forces. His research now focusses on all aspects of circuit and electromagnetic modeling of high-speed and high-frequency interconnections, on electromagnetic compatibility (EMC) and electromagnetic interference (EMI) topics and on indoor propagation. As author or co-author he has contributed to more than 60 international journal papers and 70 papers in conference proceedings.

Dr. De Zutter received the 1995 Microwave Prize Award.